

# Anomalous effect of turning off long-range mobility interactions in Stokesian Dynamics

Adam K. Townsend<sup>1, a)</sup> and Helen J. Wilson<sup>1, b)</sup>

*Department of Mathematics, University College London, Gower Street,  
London WC1E 6BT, UK*

(Dated: 16 September 2016)

In Stokesian Dynamics, particles are assumed to interact in two ways: through long-range mobility interactions and through short-range lubrication interactions. To speed up computations, in concentrated suspensions it is common to consider only lubrication. We show that, although this approximation provides acceptable results in monodisperse suspensions, in bidisperse suspensions it produces physically unreasonable results—‘bunching’—whenever external forces are applied. We suggest that this problem could be mitigated by a careful choice of particle pairs on which lubrication interactions should be included.

---

<sup>a)</sup>Electronic mail: a.townsend@ucl.ac.uk

<sup>b)</sup>Electronic mail: helen.wilson@ucl.ac.uk

## I. INTRODUCTION

The Stokesian Dynamics (SD) method<sup>4</sup> of simulating the motion of spherical particles in a Newtonian background fluid is a reliable and flexible approach to modelling low-Reynolds number suspensions. The linearity of Stokes flow allows us to relate the suspended particles' first force moments (force, torque, stresslet) to their velocity moments (velocity, angular velocity, rate of strain),

$$\begin{pmatrix} \mathbf{F} \\ \mathbf{T} \\ \mathbf{S} \end{pmatrix} = \mathcal{R} \begin{pmatrix} \mathbf{U} \\ \boldsymbol{\Omega} \\ \mathbf{E} \end{pmatrix}, \quad (1)$$

through a ‘grand resistance matrix’<sup>5</sup>,  $\mathcal{R}$ .

Although this grand resistance matrix can be generated exactly (for example, with the boundary element method), this is computationally expensive. SD provides a method to generate a good approximation to this grand resistance matrix at much less expense. For particles at large separation distances, Faxén’s laws<sup>7</sup> provide asymptotic expressions for the velocity of the surrounding fluid. These come in the inverse (‘mobility’) form to eq. (1), and fill a mobility matrix,  $\mathcal{M}^\infty$ . At short separation distances, the majority of the hydrodynamic force on a particle comes from the strong pressure gradients required to squeeze fluid out from between it and its neighbour. For interacting pairs of spheres we have full expressions for this lubrication-dominated fluid motion, and by treating all near-field interactions as pairwise, the two-body resistance matrix  $\mathcal{R}^{2\text{B},\text{exact}}$  is constructed. Since the lubrication expressions already include mobility interactions, to prevent double-counting we need to remove a mobility interaction, written in another two-body resistance matrix,  $\mathcal{R}^{2\text{B},\infty}$ . SD combines these far and near regimes to form an approximation to the grand resistance matrix which works well at all separation distances,

$$\mathcal{R}_{\text{SD}} = (\mathcal{M}^\infty)^{-1} + \mathcal{R}^{2\text{B},\text{exact}} - \mathcal{R}^{2\text{B},\infty}. \quad (2)$$

The lubrication resistance matrices,  $\mathcal{R}^{2\text{B}}$ , are typically sparse, as they are calculated only for pairs of particles which are sufficiently close together, normally with a scaled separation distance less than a critical value,  $r^*$  (also  $r_c$  in the literature),

$$\frac{2s}{a+b} < r^*, \quad (3)$$

where the centres of two particles of radius  $a$  and  $b$  are a distance  $s$  apart. A typical value<sup>3</sup> for  $r^*$  is 4. Meanwhile, the long-range mobility matrix,  $\mathcal{M}^\infty$ , considers the motion of each particle as a result of all other particles, so is always dense.

In concentrated suspensions, it is common<sup>1-3,6,8,9</sup> for simulators to assert that the motion of the particles is governed predominantly by its neighbours rather than the hydrodynamics of the system as a whole. In other words, the large number and strength of near-field lubrication forces exceeds the effect of the far-field hydrodynamic forces. In this case, researchers ‘turn off’ the dense  $\mathcal{M}^\infty$ , instead replacing it (in both the first and third terms in the right-hand side of eq. (2)) with its far-field limit: a ‘lubrication hydrodynamics’ (LH) approximation. This limit, which can be seen from Faxén’s laws as  $r \rightarrow \infty$ , consists solely of self-terms on the leading diagonal of the matrix. In particular, for identical particles of radius  $a$ , it is given by

$$\mathcal{M}_{\text{far-field limit}}^\infty = \begin{pmatrix} \frac{\mathbf{I}}{6\pi\mu a} & \mathbf{0} & \mathbf{0} \\ \mathbf{0} & \frac{\mathbf{I}}{8\pi\mu a^3} & \mathbf{0} \\ \mathbf{0} & \mathbf{0} & \frac{\mathbf{I}}{\frac{20}{3}\pi\mu a^3} \end{pmatrix}, \quad (4)$$

where  $\mathbf{I}$  is the appropriately-sized identity matrix. The viscosity term,  $\mu$ , is often replaced with an effective viscosity,  $\mu(\phi)$ , dependent on suspension concentration<sup>1</sup>. Replacing  $\mathcal{M}^\infty$  with this far-field limit gives a considerable time-saving (in our calculations, up to 50%) as the remaining grand resistance matrix,

$$\mathcal{R}_{\text{LH}} = (\mathcal{M}_{\text{far-field limit}}^\infty)^{-1} + \mathcal{R}^{2\text{B,exact}} - \mathcal{R}_{\text{far-field limit}}^{2\text{B},\infty}, \quad (5)$$

is sparse, but at the expense of accuracy.

In this paper, we examine the motion produced by this LH method of up to five close spheres in simple test cases, both monodisperse and bidisperse. Our simulations suggest that the accuracy loss for monodisperse suspensions is acceptable, but that for bidisperse suspensions, we get unphysical solutions. In particular, we find that under an external force on a large particle, small particles ‘bunch up’ in a manner which quickly leads to overlap, even at small timesteps. However, we find motion driven by an applied shear to be mostly unaffected, with a small accuracy loss. In these finite test cases, the concentration is effectively zero, so we use the unaltered solvent viscosity,  $\mu$ . The lubrication critical radius,  $r^*$ , is set to be as large as necessary so that all particle pairs are included.

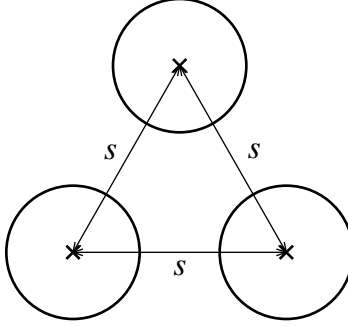


FIG. 1. Three identical spheres are arranged in an equilateral triangle with side length  $s$ , and are given a force perpendicular to the plane in which they lie.

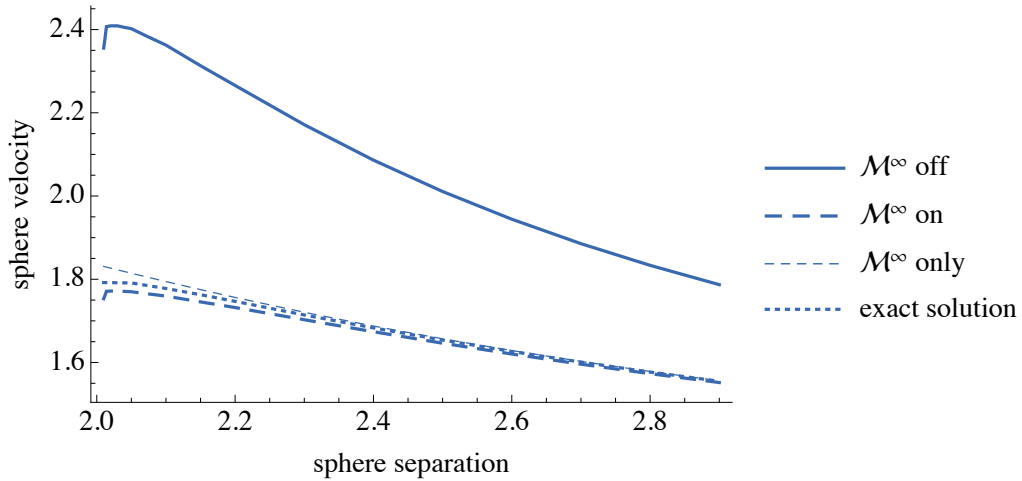


FIG. 2. Velocity of an equilateral triangle of spheres given identical forces perpendicular to their plane. The Stokesian Dynamics code with  $\mathcal{M}^\infty$  turned on matches the exact solution from the Wilson<sup>10</sup> 3-sphere code well apart from at values very close to  $s = 2$ , but the lubrication hydrodynamics method with  $\mathcal{M}^\infty$  turned off overestimates the velocity by up to 30%.

It is first worth noting that for two spheres, SD and LH methods will produce the same result, since the true  $\mathcal{M}^\infty$  matrix (term 1 in the right-hand side of eq. (2)) will match the sum over all pairwise mobility matrices (term 3 in the same equation). At higher numbers of spheres, a discrepancy grows.

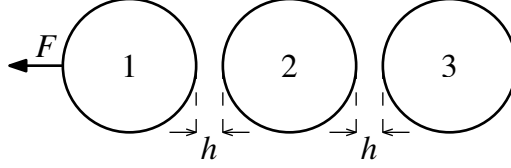


FIG. 3. Three spheres are aligned in a row, with their surfaces separated by an equal distance  $h$ . The first sphere is then given a force directly away from the other spheres.

## II. MONODISPERSE TEST CASES

We illustrate the discrepancy between using the full SD grand resistance matrix,  $\mathcal{R}_{\text{SD}}$ , ( $\mathcal{M}^\infty$  on') and the simplified far-field LH form,  $\mathcal{R}_{\text{LH}}$ , ( $\mathcal{M}^\infty$  off') with a setup from Wilson<sup>10</sup>: three identical spheres of radius  $a$ , arranged in an equilateral triangle with a given side length (see fig. 1). All three spheres are then given a force of  $6\pi\mu a$  perpendicular to the plane of the spheres. Figure 2 shows the resultant sphere velocities for both cases, and compares it with the true three-sphere velocity.

In agreement with Figure 2 in Wilson<sup>10</sup>, our SD code (with  $\mathcal{M}^\infty$  turned on) matches the exact 3-sphere solution for all separations well, with the largest error (2%) at very close sphere separations. However, the LH code (with  $\mathcal{M}^\infty$  turned off) shows much worse results, overestimating the velocity by up to 30% at the smallest separations. The results are considerably worse than those from a run with the long-range mobility matrix  $\mathcal{M}^\infty$  enabled but the lubrication matrices  $\mathcal{R}^{2\text{B},\text{exact}}$  and  $\mathcal{R}^{2\text{B},\infty}$  disabled ( $\mathcal{M}^\infty$  only'): this has an error of at most 5%. Finally, at high separations, all solutions converge.

We are now going to consider a setup of three identical, linearly aligned particles of radius  $a$ , as illustrated in fig. 3. The first particle is given a force of  $6\pi\mu a$  directly away from the other particles, and the velocities produced with  $\mathcal{M}^\infty$  both on and off are recorded in fig. 4. We see a similar phenomenon as before: turning  $\mathcal{M}^\infty$  off results in velocities for all three particles which have a similar profile shape, but whereas they converge to the exact result at high separations, at the smallest separations the readings are up to 45% larger. Once again this is worse than ignoring lubrication completely ( $\mathcal{M}^\infty$  only'), which has a maximum error of 34%.

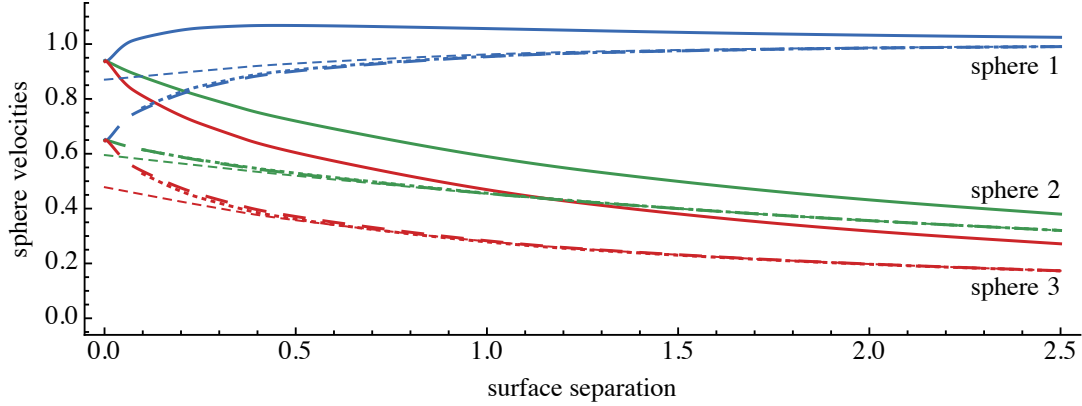


FIG. 4. Velocities of three identical particles, aligned in a row with a given, equal surface separation. The first particle is given a force directly away from the other particles and the velocities are measured with  $\mathcal{M}^\infty$  off (—) and  $\mathcal{M}^\infty$  on (– –). The exact solution from Wilson<sup>10</sup> (· · ·) is also shown, as well as with  $\mathcal{M}^\infty$  alone (– – –).

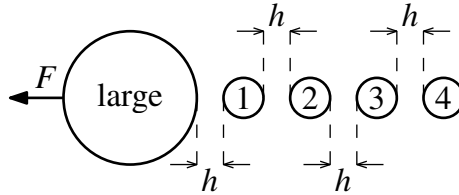


FIG. 5. A large sphere and a tail of smaller spheres are aligned in a row, with their surfaces separated by an equal distance  $h$ . The large sphere is then given a force directly away from the smaller spheres in our test cases.

### III. BIDISPERSE LINEAR TEST CASES

Although inaccurate, the 30%–45% increase in velocity seen in the monodisperse test cases is still qualitatively feasible. Since the shapes of the velocity profiles are similar, in a concentrated suspension, having many more lubrication forces, it can be argued that such local effects might ‘average out’ and would be mitigated in a concentrated suspension by use of the modified effective viscosity,  $\mu(\phi)$ . With bidisperse suspensions, however, we begin to see unphysical behaviour with  $\mathcal{M}^\infty$  turned off.

This time consider a setup of linearly aligned particles, similar to the last one, but with one large particle (of radius  $a$ ) and two small (of radius  $a/10$ ) particles, as illustrated in fig. 5 but with a shorter tail. The large particle is given a force of  $6\pi\mu a$  directly away from

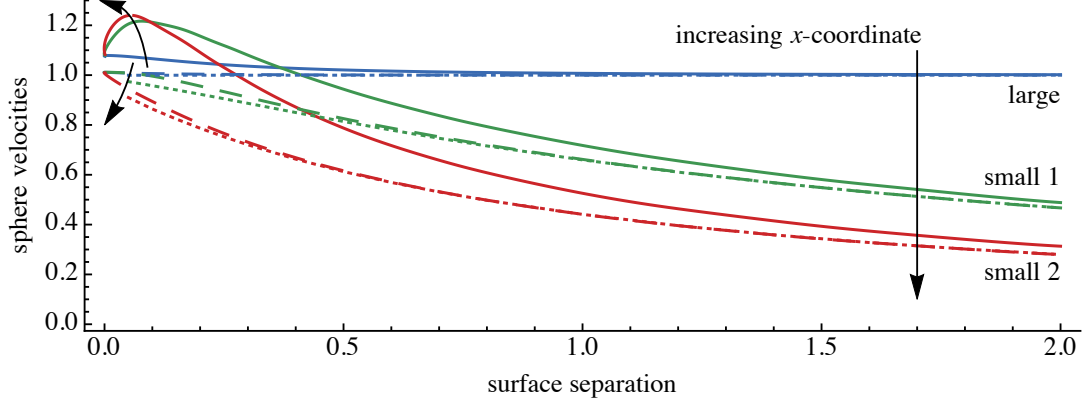


FIG. 6. Velocities of one large and two small particles, aligned in a row with a given, equal surface separation. The large particle is given a force directly away from the smaller particles and the velocities are measured with  $\mathcal{M}^\infty$  off (—) and  $\mathcal{M}^\infty$  on (---). The exact solution from Wilson<sup>10</sup> ( $\cdots$ ) is also shown. The arrows point towards the tail of the row of spheres, i.e. in the increasing  $x$ -direction.

the smaller particles and the velocities produced by SD, with  $\mathcal{M}^\infty$  on, and LH, with  $\mathcal{M}^\infty$  off, are shown in fig. 6.

For this setup, the velocity profiles for  $\mathcal{M}^\infty$  on and off no longer have the same shape. Still, at large surface separations we find convergence of the LH  $\mathcal{M}^\infty$ -off velocities to the exact result (provided by Wilson<sup>10</sup>). Full SD ( $\mathcal{M}^\infty$  on) agrees well throughout with the exact result, with errors of no more than 4% for the furthest sphere at small surface separations. However, at these close surface separations, we find the unphysical result of the small particles travelling *faster* than the sphere with the force on it. Furthermore, the small particles travel even faster the further away from the large particle they are, leading to ‘bunching’. This effect gives rise to particles overlapping at the end of the tail, as they ‘chase’ the lead particle too quickly, causing potential numerical instabilities even at small timesteps.

This result is amplified as the tail length increases. Figure 7 shows velocities for tails with three and four small particles. In the latter case, we find velocities of the small particles which are measured to be over five times larger with  $\mathcal{M}^\infty$  off than with  $\mathcal{M}^\infty$  on.

We only find this bunching effect with applied external forces. Placing the same system in an external shear produces an acceptable error between full SD and the reduced LH simulation, similar to the monodisperse case.

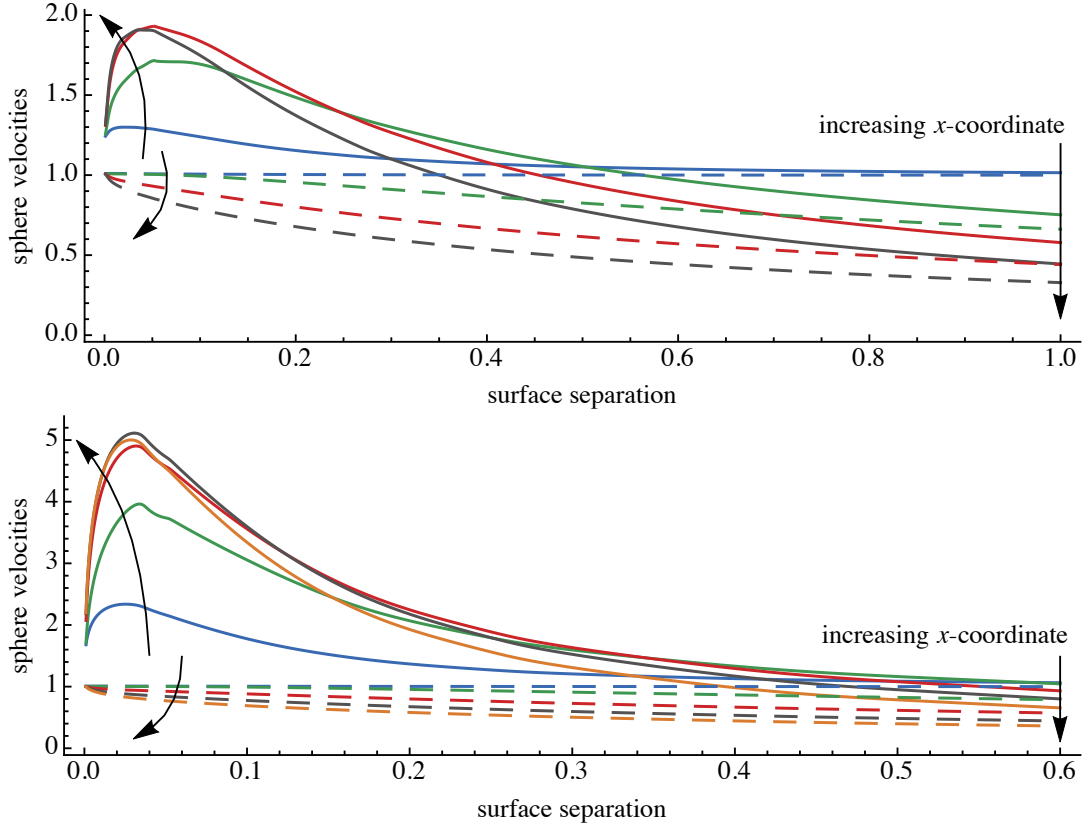


FIG. 7. *Top:* Velocities of one large and three small particles, aligned in a row with a given, equal surface separation. The large particle is given a force directly away from the smaller particles and the velocities are measured with  $\mathcal{M}^\infty$  off (—) and  $\mathcal{M}^\infty$  on (---). The arrows point towards the tail of the row of spheres, i.e. in the increasing  $x$ -direction. *Bottom:* Same but with one large and four small particles.

#### IV. MECHANISM

The mechanism we propose for the bunching behaviour seen in the previous section comes from the reach of the lubrication forces. These forces have a stronger effect on the small spheres than on the large one, and the setting of a critical radius, eq. (3), means that we can find multiple sets of lubrication interactions on the small spheres. In particular, the last small sphere in the tail feels all of these forces pulling it in the same direction, giving it a larger velocity than the others. In reality, the small spheres in between provide screening against this effect; but this is exactly what the full long-range mobility matrix  $\mathcal{M}^\infty$  captures<sup>4</sup>, which is what is lost.



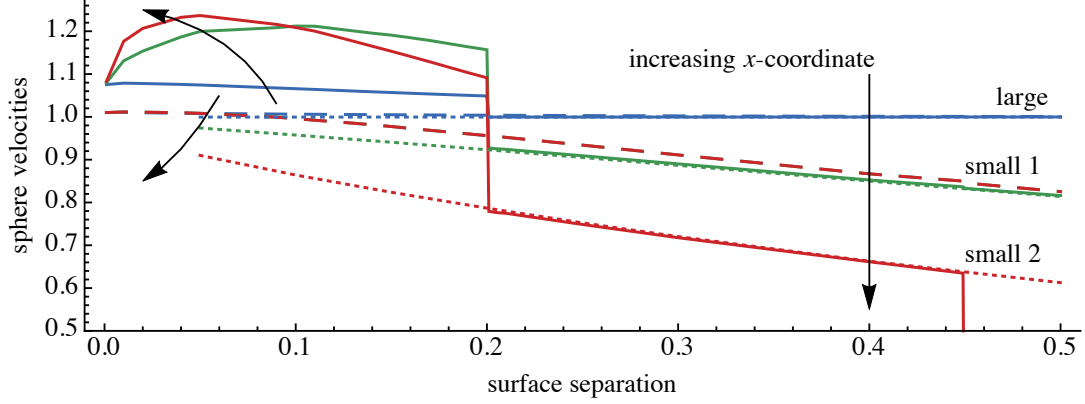


FIG. 8. The same configuration as in fig. 6, but with a reduced critical radius of  $r^* = 4$ . Velocities of one large and two small particles, aligned in a row with a given, equal surface separation. The large particle is given a force directly away from the smaller particles and the velocities are measured with  $\mathcal{M}^\infty$  off (—) and  $\mathcal{M}^\infty$  on (---). The exact solution from Wilson<sup>10</sup> (···) is also shown. The arrows point towards the tail of the row of spheres, i.e. in the increasing  $x$ -direction.

In the test cases above, the critical radius has been made sufficiently large to capture all pairwise lubrication interactions. Setting it to the previously-mentioned typical value of  $r^* = 4$  and reproducing the first test case in fig. 4 (the results of which are in fig. 6), fig. 8 shows us three distinct regions. At closest separations, all particles are within each others' critical radius, and we see the same bunching problem as before. For separations between 0.2 and 0.45, the large particle and the furthest small particle are no longer in each other's critical radius, and we see much better agreement with full SD simulations. At separations above 0.45, the furthest small particle is no longer in any other particle's critical radius and hence feels no force at all, giving it zero velocity.

The best agreement with full SD is in the central region of fig. 8. We suggest therefore, that to avoid the bunching effect while still allowing particles to feel lubrication, the LH method should be adapted to turn on lubrication only for a shell of actual nearest neighbours.

## V. CONCLUSION

Replacing the long-range mobility matrix  $\mathcal{M}^\infty$  in Stokesian Dynamics with its far-field form is shown to produce errors. For monodisperse suspensions under applied force or bidisperse suspensions under applied shear, these errors are large for small separations but

affect all the particles equally. However, for bidisperse particles under applied force, the error disproportionally affects the smaller particles, giving them unphysical velocities which, over even small timesteps, can lead to overlapping and a breakdown of the simulation. That the effect is greater with increasing numbers of particles is particularly concerning. Methods involving this lubrication hydrodynamics simplification should therefore be used with caution when applying external forces to bidisperse suspensions. We suggest that this effect can be mitigated by enabling lubrication not by measuring a critical radius, but instead only for a shell of actual nearest neighbours.

## REFERENCES

- <sup>1</sup>Tadashi Ando, Edmond Chow, and Jeffrey Skolnick. Dynamic simulation of concentrated macromolecular solutions with screened long-range hydrodynamic interactions: Algorithm and limitations. *The Journal of Chemical Physics*, 139(12):121922, September 2013. ISSN 0021-9606, 1089-7690. doi:10.1063/1.4817660. URL <http://scitation.aip.org/content/aip/journal/jcp/139/12/10.1063/1.4817660>.
- <sup>2</sup>R. C. Ball and J. R. Melrose. A simulation technique for many spheres in quasi-static motion under frame-invariant pair drag and Brownian forces. *Physica A: Statistical Mechanics and its Applications*, 247(1):444–472, December 1997. ISSN 0378-4371. doi:10.1016/S0378-4371(97)00412-3. URL <http://www.sciencedirect.com/science/article/pii/S0378437197004123>.
- <sup>3</sup>Adolfo J. Banchio and John F. Brady. Accelerated Stokesian dynamics: Brownian motion. *The Journal of Chemical Physics*, 118(22):10323–10332, June 2003. ISSN 0021-9606, 1089-7690. doi:10.1063/1.1571819. URL <http://scitation.aip.org/content/aip/journal/jcp/118/22/10.1063/1.1571819>.
- <sup>4</sup>J. F. Brady and G. Bossis. Stokesian dynamics. *Annual Review of Fluid Mechanics*, 20(1):111–157, 1988. doi:10.1146/annurev.fl.20.010188.000551. URL <http://www.annualreviews.org/doi/abs/10.1146/annurev.fl.20.010188.000551>.
- <sup>5</sup>Howard Brenner and Michael E. O’Neill. On the Stokes resistance of multiparticle systems in a linear shear field. *Chemical Engineering Science*, 27(7):1421–1439, July 1972. ISSN 0009-2509. doi:10.1016/0009-2509(72)85029-2. URL <http://www.sciencedirect.com/science/article/pii/0009250972850292>.

- <sup>6</sup>Michael D. Bybee. *Hydrodynamic Simulations of Colloidal Gels: Microstructure, Dynamics, and Rheology*. PhD Thesis, University of Illinois at Urbana-Champaign, April 2009. URL <http://hdl.handle.net/2142/11616>.
- <sup>7</sup>Sangtae Kim and Seppo J. Karrila. *Microhydrodynamics: principles and selected applications*. Dover Publications, Mineola, N.Y., 2005. ISBN 0-486-44219-5 978-0-486-44219-8.
- <sup>8</sup>Amit Kumar. *Microscale dynamics in suspensions of non-spherical particles*. PhD Thesis, University of Illinois at Urbana-Champaign, May 2010. URL <http://hdl.handle.net/2142/16032>.
- <sup>9</sup>Francisco Torres and John Gilbert. Large-Scale Stokesian Dynamics Simulations of Non-Brownian Suspensions. Technical Report C9600004, Xerox Research Centre of Canada, 1996.
- <sup>10</sup>Helen J. Wilson. Stokes flow past three spheres. *Journal of Computational Physics*, 245: 302–316, July 2013. ISSN 0021-9991. doi:10.1016/j.jcp.2013.03.020. URL <http://www.sciencedirect.com/science/article/pii/S0021999113001988>.